

204
J80 - ~~203~~

Characteristics of a Mixing Layer of a Two-Dimensional Turbulent Jet

S. Rajagopalan* and R. A. Antonia†
The University of Newcastle, New South Wales, Australia

Measurements have been made in a slightly heated or cooled mixing layer of mean and rms velocity and temperature, probability density functions, intermittency factor, spectra and convection speed of the temperature fluctuation θ . Profiles of mean and rms velocity and temperature and probability density functions of θ exhibit reasonable similarity. The boundary layer at the nozzle exit is in a state of transition and, correspondingly, the growth rate of the mixing layer is higher than that for an initially laminar boundary layer but smaller than that for an initially turbulent boundary layer. The frequency at which dominant peaks in temperature spectra occur is inversely proportional to the streamwise distance measured from the nozzle exit. The front of a turbulent bulge is found to have a larger velocity than the back.

Nomenclature

D	= width of nozzle
f	= filter cutoff frequency
f_0	= periodicity of temperature fluctuation θ near nozzle exit
f_1	= frequency at which a predominant peak occurs in θ spectrum
f_γ	= rate of occurrence of turbulent "bursts" or bulges
F	= flatness factor of $\theta \equiv \overline{\theta^4} / \overline{\theta^2}^2$
L	= integral length scale
$p(\theta)$	= probability density function of θ
$R_{\theta 0}$	= Reynolds number $U_0 \theta_0 / \nu$
S	= skewness factor of $\theta \equiv \overline{\theta^3} / \overline{\theta^2}^{3/2}$
T	= time delay, s
T_L	= integral time scale
ΔT	= difference between local mean temperature and ambient temperature
T_2	= time delay at the peak value of cross-correlation
ΔT_G	= difference between core and ambient temperatures
U	= local mean velocity
U_0	= velocity on jet centerline in the potential core
U_F	= velocity of front of turbulent bulge
U_B	= velocity of back of turbulent bulge
U_c	= convection speed estimated from cross-correlation
u	= longitudinal velocity fluctuation
u'	= rms value of $u \equiv (\overline{u^2})^{1/2}$
x	= longitudinal distance from the nozzle exit
x_0	= location of the virtual origin
y	= normal distance, measured from a line originating at nozzle tip and parallel to x axis
δ^*	= displacement thickness of boundary layer at nozzle
δ_ω	= vorticity thickness $= U_0 (dU/dy)^{-1}_{\max}$
η	= nondimensional coordinate $\equiv y / (x - x_0)$
γ	= intermittency factor or fraction of time for which flow is turbulent
ϕ	= inclination of the line of symmetry ($U = 0.5 U_0$)
$\phi(\theta)$	= spectral density function of θ
ν	= kinematic viscosity of fluid

θ	= temperature fluctuation
θ'	= rms value of $\theta \equiv (\overline{\theta^2})^{1/2}$
θ_0	= momentum thickness of boundary layer at nozzle
σ	= spread parameter of the mixing layer

I. Introduction

A DETAILED investigation of the mean and turbulent velocity field of a two-dimensional mixing layer was made by Liepmann and Laufer.¹ More recently, Wygnanski and Fiedler² and Champagne et al.³ have carried out extensive investigations of statistical properties of velocity fluctuations in a two-dimensional mixing layer. Wygnanski and Fiedler have also measured conditionally averaged turbulence quantities and the turbulent energy balance for both conventionally and conditionally averaged velocities. Spencer and Jones⁴ have studied properties of a two-stream mixing layer. By introducing heat as a passive tracer in the flow, Sunyach and Mathieu⁵ and Fiedler⁶ obtained mean and fluctuating temperature measurements, including statistical properties of the temperature fluctuation θ in a two-dimensional mixing layer. Fiedler also studied the nature of the coherent motion, transport mechanism, and entrainment. The turbulent mixing layer of a passive and chemically reacting species has been studied by Batt,⁷ who made measurements of turbulence statistics including correlations, probability density functions, skewness and flatness factors, and intermittency factor. The coherent, large-scale vortical structure has attracted considerable attention over the last few years.⁸⁻¹²

These investigations have indicated some basic differences in mixing-layer characteristics. For example, the growth rate of the mixing layer in different experiments is different, although adequate similarity is exhibited by velocity and temperature profiles when the normalizing scales are U_0 , ΔT_G , and $x - x_0$. Rodi¹³ has reviewed available data on mixing layers and suggested some plausible reasons (see Sec. III) for the observed differences. It is now believed that the initial state (laminar or turbulent) of the boundary layer at the nozzle exit plays an important role in determining some of the mixing layer characteristics. With an initially laminar boundary layer, the growth rate of the mixing layer is smaller than the growth rate with an initially turbulent boundary layer.

The main aim of the present work is to establish the turbulence characteristics of a thermal (hot and cold) mixing layer associated with a two-dimensional jet as a first step in an investigation aimed, in the longer term, at a detailed study of

Received Aug. 13, 1979; revision received Jan. 28, 1980. Copyright © American Institute of Aeronautics and Astronautics, Inc., 1980. All rights reserved.

Index categories: Jets, Wakes, and Viscid-Inviscid Flow Interactions; Boundary Layers and Convective Heat Transfer—Turbulent.

*Research Associate, Dept. of Mechanical Engineering.

†Professor, Dept. of Mechanical Engineering.

large- and small-scale structures of this layer and of the possible interaction between these structures. Measurements presented here include mean and fluctuating velocity and temperature, spectra, probability density functions, intermittency, and convection speed of θ .

II. Experimental Setup

The experimental rig consists of a P.A. Hilton Ltd. air-conditioning unit which includes a variable speed blower supplying a 25.4×25.4 cm square duct, a first heater section, a cooler section, and a second heater section followed by a 0.3 m long test section. Heating and cooling are provided by five electric elements and a conventional vapor compression unit, respectively. Downstream of the test section are a diffuser of area ratio 3/1, a settling chamber, a test section of dimensions 25.4×25.4 cm \times 1.2 m and a 2.54×25.4 cm nozzle of contraction ratio 10/1 with the longer axis vertical, all constructed of plywood. An aluminum bounding plate 1.25 cm thick, 10 cm wide, and 40 cm long with a slot of dimensions 2.54×25.4 cm is fixed at the nozzle exit. The slot has sharp edges to prevent nonuniformities at the nozzle exit and provide uniform initial conditions for the mixing layer. The nozzle exit velocity U_0 may be varied continuously from 0 to 16.1 m/s. An aluminum frame is mounted on the side of the tunnel to accommodate the traversing mechanism which consists of a modified height gage with a travel of 30 cm and a least count of 0.01 mm.

Mean and fluctuating velocity profiles were measured with the use of a nonlinearized DISA 55M01 constant temperature anemometer and a Pt-10%-Rh 5- μ m-diam hot wire operated at an overheat ratio of 0.8. Mean and fluctuating temperature profiles were measured with a 0.6 μ m Pt-10% Rh wire (length 1 mm) operated with a constant current anemometer. With a current of 0.05 mA, the sensitivity of the "cold" wire to velocity fluctuations was negligible. Both hot and cold wires were calibrated in the potential core of the jet using a Mensor quartz pressure transducer and a Comark thermocouple thermometer, respectively.

All measurements were made at the maximum exit velocity U_0 of 16.1 m/s which corresponds to a Reynolds number $U_0 D / \nu$ of 2.65×10^4 . With all heating elements switched on, ΔT_G was 28°C . With cooling conditions, ΔT_G was -8.5°C . Mean velocity and temperature measurements 0.5 mm upstream of the nozzle exit plane indicated that the flow was two-dimensional in the central 75% of the nozzle height. All measurements were made without a boundary-layer trip at the nozzle exit. Fluctuating voltages from constant-temperature and constant-current anemometers were recorded on a Hewlett-Packard 3960 FM tape recorder at a speed of 38.1 cm/s, after appropriate signal conditioning using DISA 55D26 units. The signals were later played back at 95.3 mm/s and digitized using a 10-bit A-D converter at 6400 Hz (real time). The digital data were processed on a DEC PDP 11/20 computer. Records of typically 35-s duration were used for statistical analysis.

III. Results and Discussion

Mean Velocity Field

For $1 < x/D < 4$, mean velocity profiles (Fig. 1a) exhibit good similarity. The two mixing layers meet downstream of $x/D=4$. Mixing layer growth as deduced from loci corresponding to $U=0.1, 0.5$, and $0.95 U_0$ is shown in Fig. 1b. The growth of the mixing layer is approximately linear, with the virtual origin located at the nozzle exit plane. The spread parameter σ which best fits the present data is 10.2. Comparison of values (Table 1) available in the literature indicates that there is no unique value for σ for plane mixing layers. Rodi has suggested that the difference in spread rate may depend upon one or a combination of the following:

1) The distance needed to attain full development of the mixing layer. This depends upon the initial condition, laminar

or turbulent, of the nozzle boundary layer, which would normally depend upon whether or not this boundary layer is tripped. Tripping increases the spread rate according to Fiedler and Thies.¹⁵

2) The flowfield outside the shear layer, e.g., draughts in the surroundings may influence the spread.

3) The freestream turbulence at the nozzle exit defined as $k^{1/2}/U_0$ where k is the turbulent kinetic energy.

Fiedler and Thies indicate the possibility of the existence of two types of similarity exhibited by mean velocity profiles. For a short distance from the exit, similarity depends upon initial conditions, while further downstream a universal self-preserving profile develops independently of initial con-

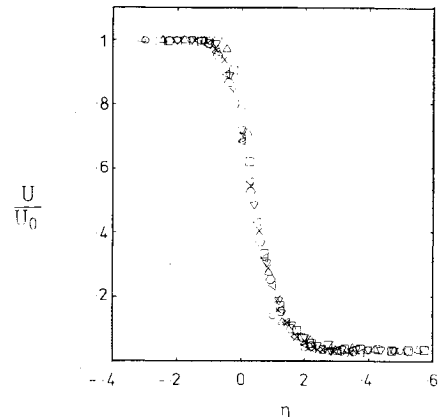


Fig. 1a Mean velocity distributions at different $x/D=1.0$, \circ , 1.5, Δ , 2 \square , 2.5 ∇ , 3 \diamond , 3.5, \times , 4 \ast .

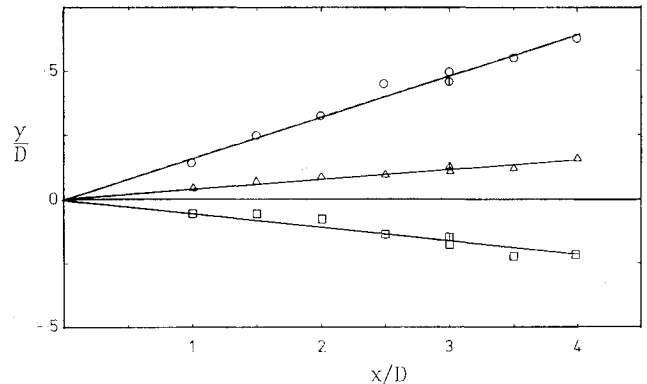


Fig. 1b Growth of velocity mixing layer: $U/U_0=0.95$, $\circ=0.5$, $\Delta=0.1$, \square at $U_0=16.1$ m/s; at points \circ, Δ, \square $U_0=8$ m/s.

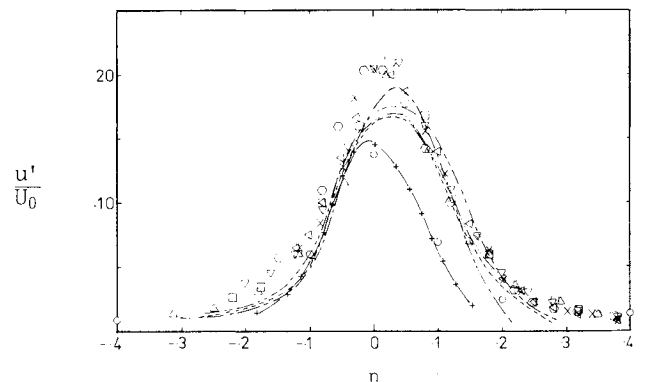


Fig. 1c Rms velocity distributions at different x/D (same legend as Fig. 1a): Laufer, $-+-+$, Sunyach and Mathieu $-----$, Wygnanski and Fiedler $----$, Champagne et al., $----$, Patel $-----$, Fiedler $-----$.

Table 1 Growth rate of mixing layer obtained by different investigators

Source	$ \tan\phi $	$\frac{y_{0.95}-y_{0.1}}{x-x_0}$	σ
Present	0.037	0.21	10.2
Champagne, et al.	0.0326	0.21	9.3
Wynanski and Fiedler ^a	0.0473	0.23	9.0
Sunyach and Mathieu	0.0361	0.192	10.1
Patel ¹⁴	0.027	0.19	10.7
Spencer and Jones	0.04	0.19	—
Liepmann and Laufer	0.03	0.17	12.0

^a Initial boundary layer tripped.

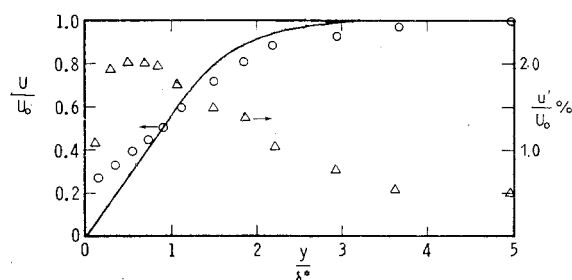
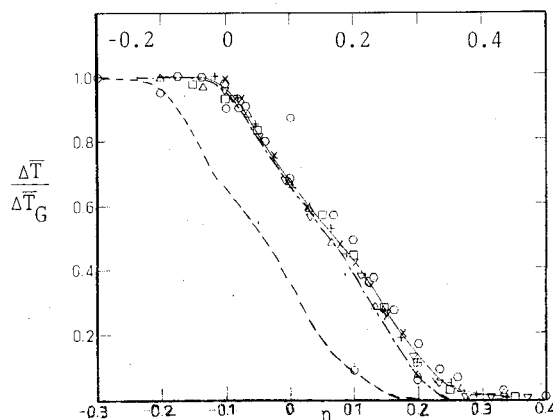
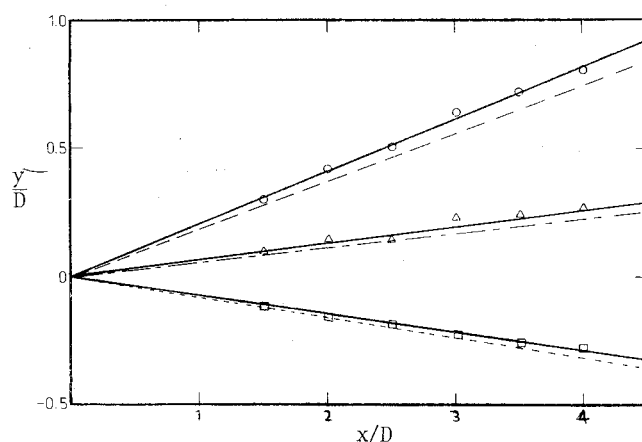
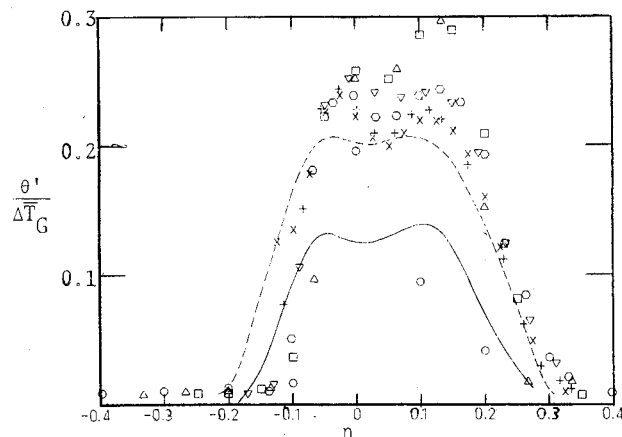
ditions. According to Champagne et al.³ the use of a boundary-layer trip at the nozzle exit influences the position of x_0 of the virtual origin. For a tripped mixing layer, x_0 occurs upstream of the exit whereas, without a trip, x_0 occurs either at the nozzle tip, as in the present case, or downstream of the tip.

The slope $\tan\phi$ of the line $U=0.5 U_0$ obtained in different mixing layer studies is given in Table 1. Keffer et al.¹⁶ observed that, for a thermal mixing layer, the plane of symmetry may be identified with $\Delta\bar{T}=0.5 \Delta\bar{T}_G$. The rms temperature and intermittency factor γ were maximum on this plane. For the velocity field, the plane of symmetry was identified with $U=0.5 U_0$; examination of u' profiles, obtained by different investigators, shows that u' is maximum on this plane. Champagne et al.³ concluded, on the basis of available results, that $0.03 < |\tan\phi| < 0.04$ for an untripped mixing layer whereas $0.04 < |\tan\phi| < 0.05$ for a tripped mixing layer. In the present case, $|\tan\phi|$ is 0.037, consistent with Champagne's conclusion. In Table 1, the state of the initial boundary layer—whether tripped or not—is also indicated. Another mixing layer growth parameter is the ratio $(y_{0.95}-y_{0.1})/(x-x_0)$ which is equal to 0.21 in the present case, in good agreement with the values of Champagne³ and Patel¹⁴ obtained without a trip. This parameter is larger for a tripped boundary layer (Table 1).

The boundary-layer velocity profile (measured at the nozzle tip with a hot wire) is transitional, the velocity profile exhibiting an inflexion point (Fig. 2). The shape factor H is 1.93 ($\delta^*=0.27$ mm, $\theta_0=0.14$ mm, and $R_{\theta_0}=145$) which is significantly smaller than that corresponding to a Blasius profile (also shown in Fig. 2), but larger than that for a turbulent boundary layer. The longitudinal turbulence intensity u'/U_0 , plotted in the same figure is maximum (0.02) at $y/\delta^*=0.60$, while the turbulence level in the core of the nozzle is about 0.5%. With an untripped boundary layer, Batt et al.¹⁷ obtained a maximum value of 0.02 for u'/U_0 with a freestream turbulence level of 0.4%. Batt⁷ suggests that σ is equal to 9 for a tripped mixing layer with a turbulent nozzle boundary layer. The present value of $\sigma=10.2$ is consistent with a boundary-layer shape which is neither laminar nor turbulent. From a study of the effect of initial conditions, Hussain and Zedan¹⁸ concluded that growth rate is almost independent of R_{θ_0} whereas it is affected by the nature (laminar or turbulent) of the initial boundary layer. Chandrsuda et al.¹⁹ have shown that the large-scale features of the mixing layer are very sensitive to the laminar or turbulent condition of the initial boundary layer. It would appear that the nature of the boundary layer exerts a major influence on σ .

Mean Temperature Field

The thermal field of a slightly heated mixing layer, in which temperature acts as a passive tracer of the flow, has not been investigated as extensively as the velocity field. Sunyach and Mathieu measured mean and fluctuating temperature, probability, and spectra of a two-dimensional thermal mixing layer. Fiedler's investigations^{6,9} concentrated mainly on the

**Fig. 2** Mean velocity and rms velocity fluctuation in nozzle boundary layer: U/U_0 , \circ ; u'/U_0 , Δ ; Blasius profile —.**Fig. 3a** Distributions of $\Delta\bar{T}/\Delta\bar{T}_G$ at different $x/D=1$, \circ , 1.5, Δ , 2, \square , 2.5, ∇ , 3, \circ , 3.5, $+$, 4, \times (heated); Fiedler ---, (cooled mixing layer)----**Fig. 3b** Growth of heated and cooled mixing layers: $\Delta\bar{T}/\Delta\bar{T}_G=0.1$, \circ , 0.5, Δ , 0.9, \square (heated); 0.9 ---, 0.5, ----, 0.1, ---- (cooled).**Fig. 3c** Distributions of rms temperature across heated mixing layer at different x/D (same legend as Fig. 3a): Sunyach and Mathieu, —, Fiedler, ----.

large-scale structure and transport mechanisms of a thermal mixing layer.

Figure 3a shows temperature distributions of $\Delta\bar{T}/\Delta\bar{T}_G$ in a heated mixing layer for different x/D . Temperature profiles become self-preserving for $x/D > 1$, in agreement with the velocity profiles. The mean temperature profile of Fiedler⁶ has also been plotted for comparison (this profile has been corrected for the difference in spread rate σ by multiplying the abscissa by the ratio of Fiedler's σ and the present value). The mean temperature profile shows three inflexion points in contrast to the velocity profile which has only one inflexion point. A similar shape for the temperature profile has been observed by Fiedler,⁶ who associated it with the presence of a large-scale vortex motion.

The growth of the thermal mixing layer is approximately linear (Fig. 3b) but its magnitude is larger than that of the velocity mixing layer. If ξ is a parameter defined such that $\xi \equiv \eta_{0.9} - \eta_{0.1}$, where $\eta_{0.9}$ and $\eta_{0.1}$ are the locations where U/U_0 (or $\Delta\bar{T}/\Delta\bar{T}_G$) are equal to 0.9 and 0.1, respectively, the ratio ξ_t/ξ_u (where subscripts t and u stand for temperature and velocity, respectively) is equal to 1.45 in the present experiment. For Sunyach and Mathieu⁵ and Fiedler,⁶ the values of this ratio are 1.7 and 1.36, respectively. The virtual origin of the present mixing layer is found to be at the nozzle exit plane (Fig. 3b). The spread is given by $|\tan\phi| = 0.068$ which is 1.84 times the value for the velocity mixing layer. Sunyach and Mathieu⁵ and Fiedler⁶ obtained 0.037 and 0.042, respectively. The growth rate of the cooled mixing layer is identical to that of the heating mixing layer (Fig. 3b). From measured values of Reynolds stress and heat flux²⁰ the average value of the turbulent Prandtl number is estimated to be 0.62 at $x/D = 2$, in close agreement with the value obtained by Batt.

Turbulence Quantities

The distribution of u' is compared (Fig. 1c) with the results of Champagne et al.,³ Wygnanski and Fiedler,² Sunyach and Mathieu,⁵ Patel,¹⁴ Liepmann and Laufer,¹ and Fiedler⁶ (all profiles corrected for σ). Present profiles of u' exhibit good similarity although the maximum value of u'/U_0 is slightly larger compared with the values available in literature. The small values of u'/U_0 in Liepmann and Laufer's experiments have been attributed (by Wygnanski and Fiedler) to the relatively poor frequency response of their anemometer. For most of the experiments the maximum value of u'/U_0 occurs at $\eta = 0.03$, which is in the plane of symmetry ($U/U_0 = 0.5$). There is apparently no universal self-preserving distribution of u'/U_0 and Champagne suggested that this lack of universality might be due to different initial and boundary conditions. In Batt's experiments,¹⁷ tripping increased u'/U_0 even though the inlet boundary layer was laminar.

The degree of similarity for θ' (Fig. 3c) is not as good for $0 < x/D < 2$ as for u' , which seems consistent with the view that temperature fluctuations require a larger distance than velocity fluctuations to reach self-preservation. Profiles of θ' exhibit two peaks, in conformity with the three inflexion points in the mean temperature profile. Fiedler's data⁶ are in satisfactory agreement with the present results, whereas Sunyach and Mathieu's values of θ' are small (both θ' profiles corrected for σ). The small θ' values of Sunyach and Mathieu could be due to the poor frequency response of the thicker wire (2 μm diameter) used by these investigators (Fiedler⁹).

Intermittency

Examination of θ traces showed that there was no region of the mixing layer which was fully turbulent even at $x/D = 4$. For $x/D < 1$, temperature fluctuations were nearly periodic at $\eta = 0$. Similar periodic fluctuations of u were noticed by Sato²¹ during studies of transition of a two-dimensional jet. As x/D increases, θ exhibits a ramp-like appearance in the central part of the mixing layer and characteristic hot or cold

spikes towards the low- and high-speed sides of the mixing layer, respectively.

The intermittency factor γ was estimated from θ traces (on a chart recorder) of 20 s duration, by measuring periods in which θ exceeded a visually prescribed threshold. The distribution of γ (Fig. 4) is in better agreement with Fiedler's⁶ results on the high- than on the low-velocity side. It is also in reasonable agreement with Batt's⁷ distribution, obtained from concentration fluctuations. It was noticed that the distribution of $f_\gamma x/U_0$ exhibited a tendency to be unique. This scaling of f_γ with x suggests that the frequency of the vortical structure, whose signature can be identified with ramps or bursts in θ , decreases like x^{-1} . This result supports Fiedler's⁹ observation, based upon dimensional arguments, that the frequency of the coherent large vortex in a two-dimensional mixing layer varies as x^{-1} .

Probability Density Functions of Temperature

At $x/D = 0.5$ and 0.75 , where θ is almost periodic, the probability density function (pdf) of θ (Fig. 5a) for $\eta = 0$ is slightly negatively skewed. At $x/D = 0.75$ the pdf becomes bimodal; one of the peaks is associated with turbulent temperature fluctuations and the other with hot (or cold) potential core fluid. The pdf associated with the hot or cold potential core fluid should ideally be a delta functions, but is nearly Gaussian due to electronic noise and low-frequency temperature fluctuations in the potential core. As x/D increases, the bimodal shape can be observed only at large positive or negative values of η , but the magnitude of the peak associated with the potential core or ambient temperature is only small compared with that of the peak corresponding to the hot or cold spikes. In the central part of the mixing layer, the pdf has a trimodal shape (Fig. 5b), the three peaks being associated with potential core fluid, turbulent temperature fluctuations, and ambient room fluid. The skewness S and flatness factor F of θ indicated that S is negative for $\eta \leq 0.02$ and positive for $\eta > 0.02$. Both S and F are large at the edges of the mixing layer, as a result of the highly intermittent appearance of θ in this region.

Turbulence Spectra

Figure 6 shows one-dimensional spectra of θ at $x/D = 2$ and 4 for the heated layer. It was noticed that at $x/D = 0.5$ and 0.75 , these spectra exhibited a sharp peak at a frequency f_θ of about 1.05 kHz at $\eta = 0$. This is consistent with the quasiperiodic appearance of θ (visual examination gave

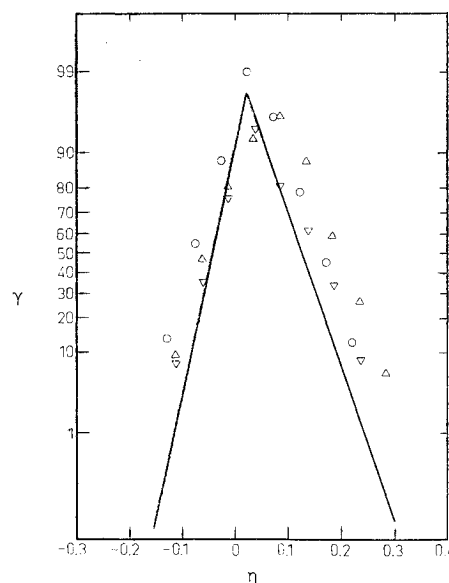


Fig. 4 Distributions of intermittency factor γ and f_γ (γ plotted on probability paper): $x/D = 1$ \square , 2 ∇ , 3 Δ , 4 \circ , Fiedler —.

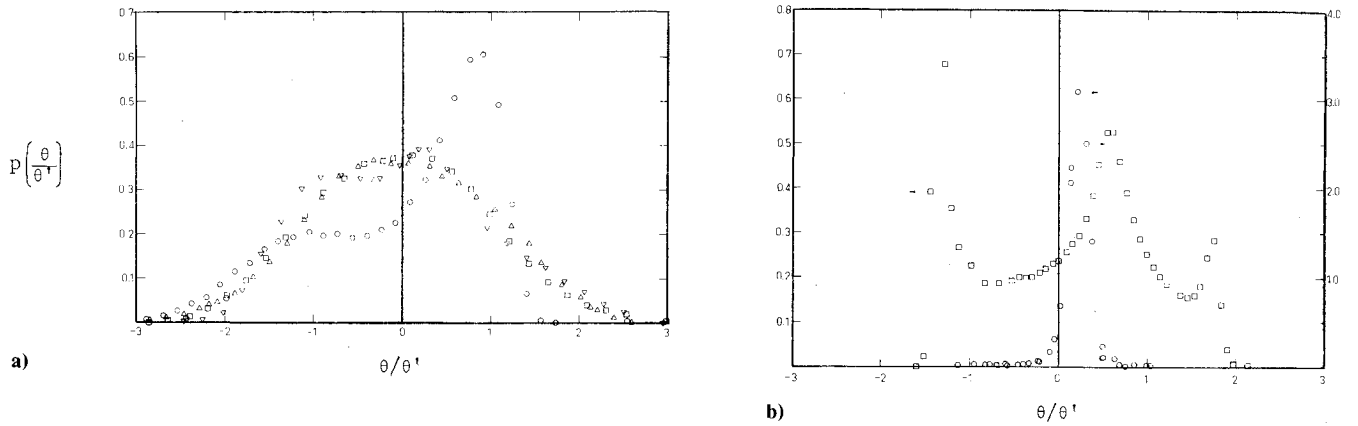


Fig. 5 Distributions of probability density function of θ : a) $\eta = 0$; $x/D = 0.5$ (heated) Δ , 0.75 (heated) \circ , 0.5 (cooled) \square , 0.75 (cooled) ∇ . b) $x/D = 2$ (heated), $\eta = -0.1$ \circ , 0.1 \square , 0.3 \diamond .

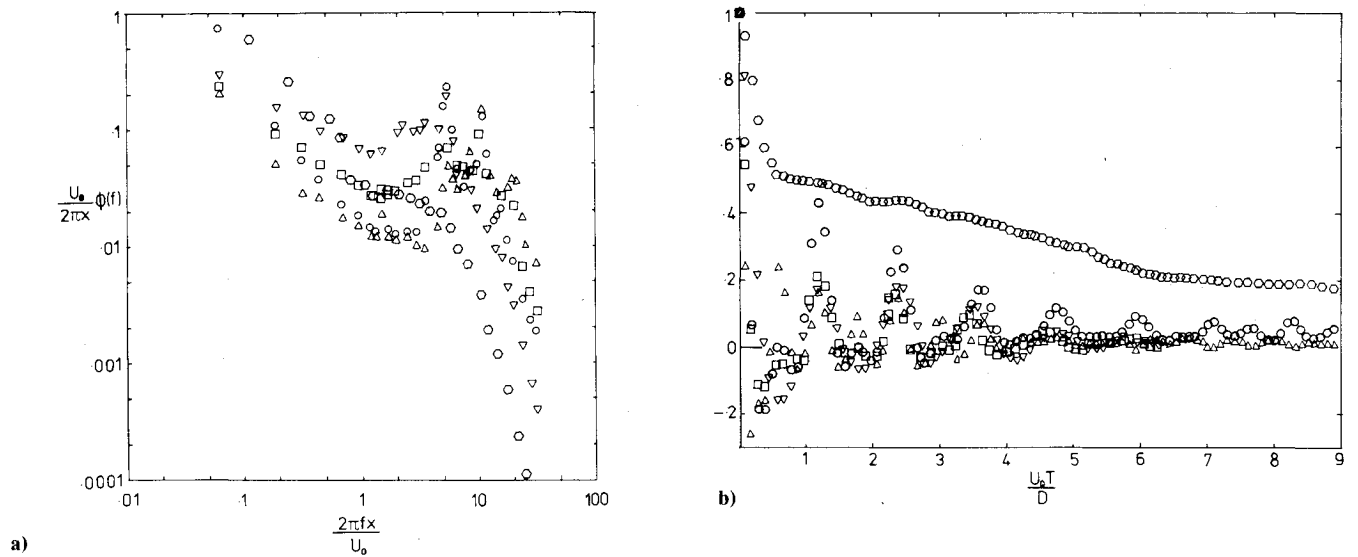


Fig. 6 a) Spectra of temperature; b) autocorrelations of temperature. $x/D = 2.0$ (heated); $\eta = -0.1$ \circ , -0.05Δ , 0 \square , 0.05 ∇ , 0.1 \diamond .

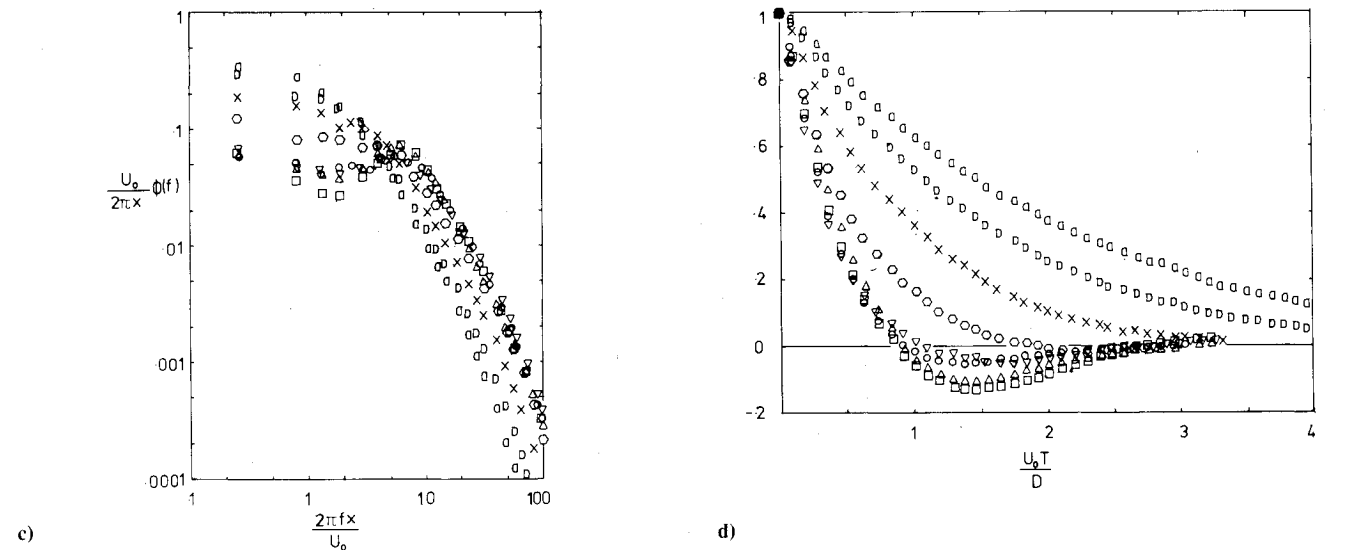


Fig. 6 c) Spectra of temperature; d) autocorrelations of temperature. $x/D = 4$, $\eta = -0.125$ \circ , -0.075Δ , -0.025 \square , 0 \circ , 0.075 \diamond , 0.0125 \times , 0.175 \square , 0.0225 \diamond .

frequency of 1.06 kHz). The Strouhal number $St = f_0 D / U_0$ is 1.65. During a study of breakdown of plane jets, Rockwell and Nicolls²² observed that the Strouhal number based upon the frequency of formation and breakdown of vortices varied as $St = 0.012 R^{0.5}$, where R is the Reynolds number based

upon average exit velocity and nozzle width. For the present Reynolds number, $St = 1.9$, which is in reasonable agreement with the observed value of 1.65. Within the potential core of a high-speed circular jet where Ko and Davies²³ observed peaks in the spectra of velocity fluctuations and on the jet axis, St

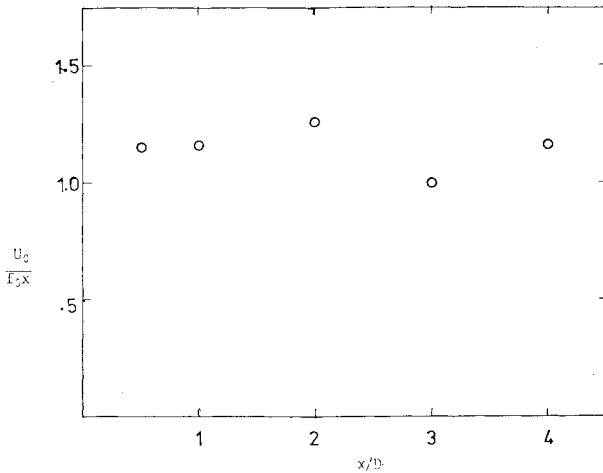


Fig. 7 Streamwise variation of frequency of dominant peak in temperature spectrum, $-0.1 < \eta < 0$.

varied from 0.47 to 0.56 as the exit Mach number changed from 0.06 to 0.37. They also observed that at $x/D=0.75$, St increased from 0.57 on the centerline to 1.4 at $\eta=0.4$ before decreasing with a further increase in η .

As x/D increases, the frequency f_0 of the spectral peak decreases and is mainly noticeable on the high-speed side of the mixing layer. Such a decrease in f_0 was noted by Yule²⁴ and Hussain and Clark.²⁵ At $x/D=1$, a prominent peak in the θ spectrum occurs at 550 Hz ($f_0 D/U_0=0.86$), and a milder peak is observed at 1.05 kHz for $\eta=-0.1$, -0.05 , and 0. Visual inspection of θ at these values of η indicated a dominant frequency of about 550 Hz and the presence of high-frequency harmonics. Although two or occasionally three peaks are exhibited by the spectra, as x/D increases the frequency f_0 at which the dominant peak occurs decreases approximately as x^{-1} (Fig. 7). This seems consistent with the amalgamation of large-scale vortical structures and the observation of Fiedler⁹ that the frequency of occurrence of large-scale structures varies as x^{-1} . Unlike the present results, Batt⁷ did not observe a peak in spectra of θ in the mixing region.

Autocorrelation curves plotted in Fig. 6 against the non-dimensional time delay $U_0 T/D$, where T is the time delay, suggest that large eddies dominate the outer part of the mixing layer as x/D increases. The integral time scale T_I was calculated by computing the area, to the first zero crossing, under the autocorrelation curves at $\eta=-0.15$ and 0.10 for $1.5 < x/D < 4$. The integral length scale L obtained by multiplying T_I by either U_0 or U_c is plotted in Fig. 8. (It is assumed that U_c/U_0 exhibits similarity.) For $x/D > 1$, L grows approximately linearly. A linear growth of the integral length scale was noted by Batt. Davies et al.²⁶ found that integral length scale grows linearly in the potential core region, on the axis of a circular jet. Dimotakis and Brown¹¹ observed that in a two-stream mixing layer $3.1 < \ell/\delta_\omega < 5$ where the length scale ℓ was obtained by multiplying the convection speed by twice the time corresponding to the first minimum of the u autocorrelation. For the present experiments ℓ/δ_ω varies from 5.4 at $x/D=2$ to 2.7 at $x/D=4$, in close agreement with the results of Dimotakis and Brown.

Convection Speed

The convection speed U_c of θ was measured at $x/D=3$, using two cold wires separated longitudinally by a distance $\Delta x=0.85$ cm. Because of the intermittent nature of θ convection speeds U_F and U_B , associated with the "front" and "back," respectively, of a turbulent bulge were determined by first recording the two θ traces on a chart recorder and estimating, by visual inspection, the average time delay between arrivals of fronts (or backs) at the positions of the

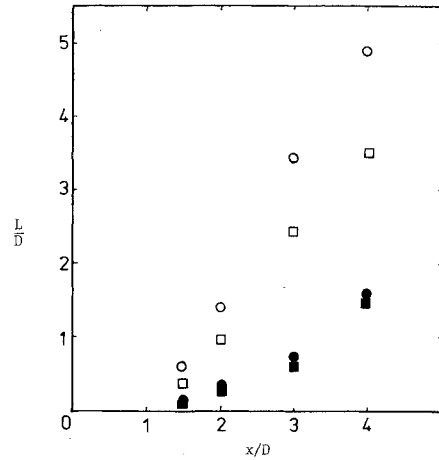


Fig. 8 Integral length scale L : $\eta=0.1$ \circ , -0.15 \bullet (L estimated as $L=U_0 T_I$ where T_I is integral time scale), $\eta=0.1$ \square , -0.15 \blacksquare , $L=U_c T_I$.

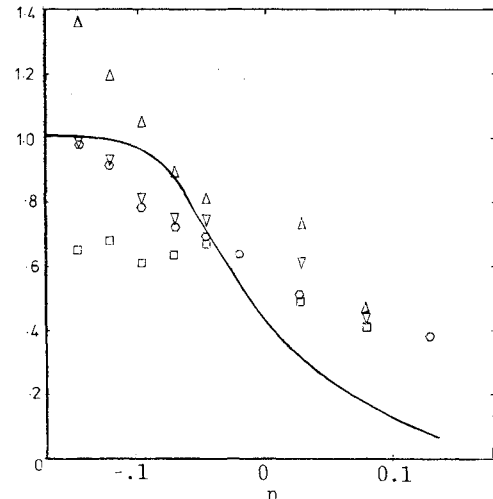


Fig. 9 Convection speed estimated using different techniques ($x/D=3$, $\Delta x/D=0.33$): U_F/U_0 Δ , U_B/U_0 \square , $(U_F + U_B/2)/U_0$ ∇ , U_c/U_0 \circ , U_c obtained from cross-correlation, U/U_0 —.

wires. For $\eta < -0.05$ the front moves at approximately $0.65 U_0$ (Fig. 9). From space-time correlations of θ , the average time delay T_2 corresponding to the peak in the correlation curve was determined and the convection speed U_c obtained from the ratio $\Delta x/T_2$.[‡] The agreement between U_c and U_{av} ($\equiv (U_F + U_B)/2$) is satisfactory toward the high-speed side of the layer. For $\eta > 0.5$, estimates of U_F and U_B become less reliable because of the highly intermittent character of θ . Ko and Davies²³ observed that, in the mixing region of a circular jet, U_c/U_0 decreased from nearly 0.75 at the edge of the potential core as y increased. (Their study concentrated mainly on the potential core and only a few measurements were made in the mixing layer.) Within the potential core, U_c/U_0 increased from 0.62 on the jet axis to about 0.75 at the edge.

IV. Summary of Results

Some of the characteristics of a slightly heated or slightly cooled mixing layer may be summarized as follows:

1) Mean velocity and temperature profiles are approximately similar for $x/D > 1.5$. The rms velocity is more nearly self-preserving than the rms temperature.

[‡]The effect on U_c of low-pass and band-pass filtering θ at $x/D=2.7$ and $\eta=0.1$ was investigated. U_c was found to be independent of filter frequency f for $fD/U_0 > 0.32$ for both low-pass and band-pass filters; U_c decreased with f for $fD/U_0 < 0.32$. Batt also noticed a similar effect of filter frequency on U_c .

2) The rate of growth of the mixing layer seems consistent with the transitional nature of the boundary layer at the nozzle exit.

3) Probability density functions of θ exhibit either a bimodal or trimodal shape, depending upon the position in the layer.

4) Temperature spectra exhibit a peak on the high-speed side of the layer. The dominant frequency corresponding to this peak varies approximately as x^{-1} . The nondimensional frequency of occurrence of turbulent bulges also varies approximately as x^{-1} . Turbulence integral length scales grow nearly linearly with distance but their magnitude is larger near the low-speed than toward the high-speed side of the layer.

5) The front of a turbulent "bulge" moves faster than the back. On the high-speed side, the convection speed of the front is larger than that of the jet exit velocity.

Acknowledgment

The support of the Australian Research Grants Committee is gratefully acknowledged.

References

- ¹Liepmann, H. W. and Laufer, J., "Investigations of Free Turbulent Mixing," NACA TN 1257, 1947.
- ²Wynanski, I. and Fiedler, H. E., "The Two Dimensional Mixing Region," *Journal of Fluid Mechanics*, Vol. 41, Pt. 2, 1970, pp. 327-361.
- ³Champagne, F. H., Pao, Y. H., and Wynanski, I. J., "On the Two Dimensional Mixing Region," *Journal of Fluid Mechanics*, Vol. 74, Pt. 2, 1976, pp. 209-250.
- ⁴Spencer, B. W. and Jones, B. G., "Statistical Investigation of Pressure and Velocity Fields in the Turbulent Two-Stream Mixing Layer," AIAA Paper 71-613, June 1971.
- ⁵Sunyach, M. and Mathieu, J., "Zone de Mélange d'un Jet Plan: Fluctuations Induites dans le Cône a Potentiel—Intermittence," *International Journal of Heat and Mass Transfer*, Vol. 12, Dec. 1969, pp. 1679-1697.
- ⁶Fiedler, H. E., "Transport of Heat Across a Plane Turbulent Mixing Layer," *Advances in Geophysics*, Vol. 18A, 1974, pp. 93-109.
- ⁷Batt, R. G., "Turbulent Mixing of Passive and Chemically Reacting Species in a Low Speed Shear Layer," *Journal of Fluid Mechanics*, Vol. 82, Pt. 1, 1977, pp. 53-95.
- ⁸Brown, G. L. and Roshko, A., "On Density Effects and Large Structure in Turbulent Mixing Layers," *Journal of Fluid Mechanics*, Vol. 64, Pt. 4, 1974, pp. 775-816.
- ⁹Fiedler, H. E., "On Turbulence Structure and Mixing Mechanism in Free Turbulent Shear Flows," *Turbulent Mixing in Reactive and Non Reactive Flows*, edited by S.N.B. Murthy, Plenum Press, New York, 1975, pp. 381-407.
- ¹⁰Browand, F. K. and Weidman, P. D., "Large Scales in Developing Mixing Layer," *Journal of Fluid Mechanics*, Vol. 76, Pt. 1, 1976, pp. 127-144.
- ¹¹Dimotakis, P. E. and Brown, G. L., "The Mixing Layer at High Reynolds Number: Large Structure Dynamics and Entrainment," *Journal of Fluid Mechanics*, Vol. 78, Pt. 3, 1976, pp. 535-560.
- ¹²Winant, C. D. and Browand, F. K., "Vortex Pairing: The Mechanism of Turbulent Mixing Layer Growth at High Reynolds Number," *Journal of Fluid Mechanics*, Vol. 63, Pt. 2, 1974, pp. 237-255.
- ¹³Rodi, W., "A Review of Experimental Data of Uniform Density Free Turbulent Boundary Layers," *Studies in Convection: Theory, Measurement and Applications*, edited by B. E. Laufer, Academic Press, New York, 1975, pp. 79-165.
- ¹⁴Patel, R. P., "An Experimental Study of a Plane Mixing Layer," *The Physics of Fluids*, Vol. 11, Jan. 1973, pp. 67-71.
- ¹⁵Fiedler, H. and Thies, H. J., "Some Observations in a Large Two-Dimensional Shear Layer," *Structures and Mechanics of Turbulence*, Vol. 1, edited by H. Fiedler, *Lecture Notes in Physics*, Springer Verlag, New York, 1978, pp. 108-117.
- ¹⁶Keffer, J. F., Olsen, G. J. and Kanwall, J. G., "Intermittency in a Thermal Mixing Layer," *Journal of Fluid Mechanics*, Vol. 79, Pt. 3, 1977, pp. 595-607.
- ¹⁷Batt, R. G., Kubota, T., and Laufer, J., "Experimental Investigation of the Effect of Shear-Flow Turbulence on a Chemical Reaction," AIAA Paper 70-271, June 1970.
- ¹⁸Hussain, A.K.M.F. and Zedan, M. F., "Effects of the Initial Condition on the Axisymmetric Free Shear Layer: Effects of the Initial Momentum Thickness," *The Physics of Fluids*, Vol. 21, No. 7, 1978, pp. 1100-1112.
- ¹⁹Chandrsuda, C., Mehta, R. D., Weir, A. D. and Bradshaw, P., "Effect of Free Stream Turbulence on Large Structure in Turbulent Mixing Layers," *Journal of Fluid Mechanics*, Vol. 85, Pt. 4, 1978, pp. 693-704.
- ²⁰Rajagopalan, S. and Antonia, R. A., "Properties of the Large Structure in a Slightly Heated Turbulent Mixing Layer," Dept. of Mechanical Engineering, University of Newcastle, Rept. FM 44, 1979.
- ²¹Sato, H., "The Stability and Transition of a Two Dimensional Jet," *Journal of Fluid Mechanics*, Vol. 7, Pt. 1, 1959, pp. 53-80.
- ²²Rockwell, D. O. and Nicolls, W. D., "Natural Breakdown of Planar Jets," *Transactions of ASME, Journal of Basic Engineering*, Vol. 94, Dec. 1972, pp. 720-730.
- ²³Ko, N.W.M. and Davies, P.O.A.L., "The Near Field Within the Potential Core of Subsonic Cold Jets," *Journal of Fluid Mechanics*, Vol. 50, Pt. 1, 1971, pp. 49-78.
- ²⁴Yule, A. J., "Large-Scale Structure in the Mixing Layer of a Round Jet," *Journal of Fluid Mechanics*, Vol. 89, Pt. 3, 1978, pp. 413-432.
- ²⁵Hussain, A.K.M.F. and Clark, A. R., "On the Coherent Structure of the Axisymmetric Mixing Layer: A Flow Visualization Study," Aerodynamics and Turbulence Laboratory, Univ. of Houston, Rept. FM-6, 1979.
- ²⁶Davies, P.O.A.L., Fisher, M. J., and Barratt, M. J., "The Characteristics of the Turbulence in the Mixing Region of a Round Jet," *Journal of Fluid Mechanics*, Vol. 15, Pt. 3, 1963, pp. 337-367.